中国光学（中英文）
Chinese Optics
核心期刊

A highly efficient terahertz amplitude modulator based on the phase transition of MoS_2

SHEN Yan-chun, HE Zhen-wu, LUO Zhuo-bin, PAN Guan-quan, ZHAN Pei-yi, WEI Dong-shan, ZHAO Yi-liang

Citation:
SHEN Yan-chun, HE Zhen-wu, LUO Zhuo-bin, PAN Guan-quan, ZHAN Pei-yi, WEI Dong-shan, ZHAO Yi-liang. A highly efficient terahertz amplitude modulator based on the phase transition of MoS_2[J]. *Chinese Optics*, In press. doi: 10.3724/CO.EN-2026-0023
申彦春, 何镇武, 罗卓彬, 盘关泉, 詹佩怡, 魏东山, 赵以亮. 基于二硫化钼相变的高效太赫兹振幅调制器[J]. 中国光学, 优先发表. doi: 10.3724/CO.EN-2026-0023

View online: https://doi.org/10.3724/CO.EN-2026-0023

文章编号　2097-1842(xxxx)x-0001-09

A highly efficient terahertz amplitude modulator based on the phase transition of MoS_2

SHEN Yan-chun[1], HE Zhen-wu[1], LUO Zhuo-bin[1], PAN Guan-quan[1], ZHAN Pei-yi[1], WEI Dong-shan[2*], ZHAO Yi-liang[3]

(1. *School of Railway Transportation*, *Guangzhou Railway Polytechnic*, *Guangzhou* 511300, *China*;
2. *School of Physics and Electronic Engineering*, *Hainan Normal University*, *Haikou* 571158, *China*;
3. *Xining Communication Section*, *China Railway Qingzang Group Co.*, *Ltd.*, *Xining*, *China*, 810007)
* *Corresponding author*, *E-mail*: *dswei@hainnu.edu.cn*

Abstract: Terahertz (THz) wave modulation via metasurfaces exhibits considerable applications in THz communications, imaging, and detection. In this study, a molybdenum disulfide (MoS_2) metasurface is proposed to realize THz amplitude modulation at very low trigger voltages. The unit micro-nanostructure is characterized by a broken "H" shape linked by a MoS_2 layer. Simulation results indicate that the electrical control of the phase transition at the "H" junction can enable substantial amplitude modulation at 0.58 THz with a modulation rate of 98% and a low insertion loss of 20%. The modulation mechanism is elucidated by analyzing the electric field distributions at different structural positions and the diffraction patterns before and after the phase transition. To verify the design, electrical measurements in experiment are carried out on a MoS_2 layer with the same thickness of 2 μm and the resistivity of the measured MoS_2 layer varied by nearly six orders of magnitude with a minor change of the low trigger voltage from 0 to ±1 V, validating the feasibility of the interfacial metasurface control. This study is anticipated to offer a novel method for THz amplitude modulation, and promote the practical development of THz modulation devices.

Key words: terahertz modulator; molybdenum disulfide (MoS_2); metasurface; phase transition; low trigger voltage; diffraction pattern

收稿日期:2026-06-03; **修订日期:**xxxx-xx-xx
基金项目:国家自然科学基金 (No. 62475276, No. 12204457)
Supported by National Natural Science Foundation of China (No. 62475276, No. 12204457)

基于二硫化钼相变的高效太赫兹振幅调制器

申彦春[1], 何镇武[1], 罗卓彬[1], 盘关泉[1], 詹佩怡[1], 魏东山[2*], 赵以亮[3]
（1. 广州铁路职业技术学院轨道交通学院, 广州 511300;
2. 海南师范大学物理与电子工程学院, 海口 571158;
3. 中国铁路青藏集团有限公司西宁通信段, 西宁 810007）

摘要: 基于超表面的太赫兹(THz)波调控在太赫兹通信、成像及探测领域具有重要应用价值。本研究提出一种二硫化钼(MoS_2)超表面结构, 可在极低驱动电压下实现太赫兹振幅调制,其单元微纳结构为二硫化钼层连接的非对称“H”型。仿真结果表明, 通过电控调控“H”型连接处的相变, 该调制器可在 0.58 THz 处实现大幅振幅调制, 调制深度达 98%, 插入损耗低至 20%, 其调控机理可通过分析相变前后不同结构位置的电场分布与衍射图样得到解释。为验证设计方案, 对厚度为 2 μm 的二硫化钼薄膜进行电学测试, 结果显示: 在 0~±1 V 的低驱动电压小幅变化下, 二硫化钼薄膜电阻率变化近 6 个数量级, 证实了界面型超表面调控的可行性。本研究可为太赫兹振幅调制提供一种新方法, 有望推动太赫兹调控器件的实用化发展。

关 键 词: 太赫兹调制器; 二硫化钼 (MoS_2); 超表面; 相变; 低驱动电压; 衍射图样
中图分类号: O436 **文献标志码:** A **doi:** 10.3724/CO.EN-2026-0023 **CSTR:** 32171.14.CO.EN-2026-0023

1 Introduction

Optical modulators are widely employed in contemporary telecommunication systems to regulate beam parameters, encompassing amplitude[1-3], phase[4], frequency[5], and polarization[6-8]. The escalating requirements for high data rate wireless networks[9], quantum communication capacities[10], and quantum key distribution[11] have substantially expedited the advancement of modulation technologies utilizing all-optical devices and circuits[12], facilitating advanced communication within the visible and microwave spectra.

Terahertz (THz) waves (ranging from 0.1 to 10 THz) exhibit far - reaching significance for multiple disciplines, including molecular biology, medical imaging, security detection, and next-generation communication systems[4, 13-19]. Functional devices operating in the THz frequency range, such as filters[20], polarizers[21-22], and modulators[23-26], are crucial for the progress of applications related to spectroscopy, imaging, and communication. As fundamental constituents for THz wave modulation. THz intensity modulators are among the most crucial functional devices.

Recent research has reported a variety of THz modulation techniques. Wu et al.[27] demonstrated the high-performance characteristics of THz modulators fabricated using a sandwich structure based on ionic liquids (ILs) and graphene. When a 3 V gate voltage is applied, these modulators can achieve a bandwidth coverage ranging from 0.1 to 2.5 THz, with a modulation depth up to 99%. Nevertheless, such transmission wave modulation devices manifest significant insertion loss[28]. Chen et al.[29] developed a superior THz modulator that exploits the conductivity variations of graphene to attain up to 99.6% reflection modulation. By electronically exciting graphene to regulate its conductivity, the device modulates the Brewster angle for high phase and signal modulation. However, its operation is dependent on the Brewster angle, leading to relatively high insertion loss, which renders it impractical for real world applications. Gaspare et al.[30] proposed a gate-adjustable single-layer graphene modulator operating within the 2-5 THz range. By integrating graphene into a quarter-wave cavity and utilizing an ionic liquid gate, an amplitude modulation depth of 40% was attained. These investigations indicate that the performance of modulation devices is seriously limited by the insertion loss and modulation depth.

Metasurfaces, which are two dimensional nanostructured surfaces, facilitate multifunctional wavefront-controlled light and are pivotal in regulating the amplitude, phase, and polarization of reflected/transmitted light[31-35]. In addition to being notably thinner than conventional optical components, metasurfaces demonstrate sensitivity to alteration to the dielectric environment, especially the alteration triggered by resonance[36]. Sensitivity of the metasurfaces can be further augmented through the design of plasmon resonance fields. One strategy to enhance adjustability of the metasurfaces is to combine plasmonic metasurfaces with active materials. By meticulously designing unit micro/nanostructures and selecting suitable tunable materials, dynamic regulation of light fields (e.g., phase and amplitude) can be realized[37]. Commonly employed tunable materials include liquid crystals[38-40], conductive oxide materials[41], two-dimensional materials[42] and phase-change materials[43]. In 2024, Xiao et al.[44] demonstrated that the printed Ag/MoS_2/Ag heterostructures can function as zero-electrostatic switches for the radiofrequency/microwave spectrometers and fully integrated reconfigurable metasurfaces. When combined with graphene, the device facilitates reconfigurable metasurfaces for electromagnetic wave manipulation, wireless communication, sensing, and hologram control. In their study, the molybdenum disulfide (MoS_2) layer exhibits a resistance variation of seven orders of magnitude at low trigger voltage, indicating a phase transition of MoS_2 from an insulating state to a conducting state. Phase-transition in active materials (predominantly VO_2, chalcogenide, 2D materials, etc.) via heat, voltage or light drastically alters the material's complex permittivity and conductivity, which either modulates the optical path of propagating THz waves in thin films or reconfigures resonant conditions of integrated metasurface microstructures. The resulting shift in wave interference, surface impedance and resonant dispersion produces large, tunable phase and amplitude variations of transmitted or reflected THz signals, with switching speed governed by carrier excitation, electron-phonon coupling and lattice rearrangement kinetics of the phase-change medium. In 2024, Hu et al.[45] put forward a terahertz amplitude reflection modulation device via P-N junction carrier mobility modulation and attained a relative phase modulation of 270° and a reflection efficiency of 30% under the electrical control. This significant advancement inspires the application of MoS_2 layers in the design of dynamic metasurfaces. By leveraging the resonant properties of these structures, it is possible to fabricate amplitude modulators with low insertion loss and high modulation efficiency.

In this research, a dynamic metasurface amplitude modulator based on the electro-controlled phase transition of MoS_2 is developed and the efficient THz amplitude modulation at low driving voltages while keeping the insertion loss at a low level is verified by finite element simulations. The modulation and the performance improvement mechanisms of the metasurface are explained and discussed according to the phase transition of MoS_2 layers at low trigger voltages. The proposed electro-controlled metasurface design is anticipated to offer innovative methodologies for the development of terahertz amplitude modulation systems.

2 Model

Figure 1 presents a schematic of our designed metasurface micro-nano unit structure and the electrically tunable grating developed using this design. The metasurface consists of silver nanoelectrodes and a MoS_2 layer with a thickness of 2 μm, including a phase change region under the electrical control highlighted by a red dashed square. The MoS_2 phase transition can be triggered by the formation of silver conductive wires during electrical modulation[44], ensuring the phase change occurs exclusively in the silver wire-formed areas. Although MoS_2 coating covers the entire metasurface, phase transitions are confined to the interelectrode gaps between the silver electrodes. Each electrode row in the transmissive modulation grating operates independently with a 120-μm period. Through the voltage control, individual rows can be precisely modulated to adjust the transmission amplitude of the incident terahertz wave, creating an amplitude grating that modulates both the diffraction direction and the order of transmitted light.

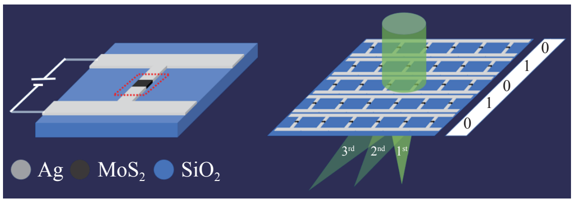

Fig. 1 Schematic of the metasurface's micro-nano unit structure (the red square marks the phase transition region) and a demonstration of its transmission modulation application.

3 Experiment results

3.1 Electrical-controlled phase transition measurements of MoS_2

To ensure the function of the designed THz modulator, the electrical-controlled phase transition of MoS_2 is crucial. As shown in Fig. 2a, an electrical-controlled phase transition test using a data source table with two disconnected silver electrodes and a drop-coated MoS_2 thick layer (Fig. 2b) is performed. The resistance-voltage curve of the MoS_2 layer under electrical control is displayed in Fig. 2c. When the voltage varies from 0 to -1.1 V, the inverse of MoS_2 resistance rises from 5×10^{-5} Ω^{-1} to 0.5 Ω^{-1}, indicating the transition of MoS_2 from the 2H state to the 1T state. When the voltage varies from −1.1 to 1.0 V, the resistance remained stable, demonstrating MoS_2 remains 1T state under the voltage variation. Beyond 1.0 V, the inverse resistance decreased to 5×10^{-5} Ω^{-1}, confirming MoS_2 returns to the 2H state, as observed in the literature[44]. This phenomenon not only illustrates the electrical-controlled phase transition process but also validates the feasibility of such phase transitions of MoS_2.

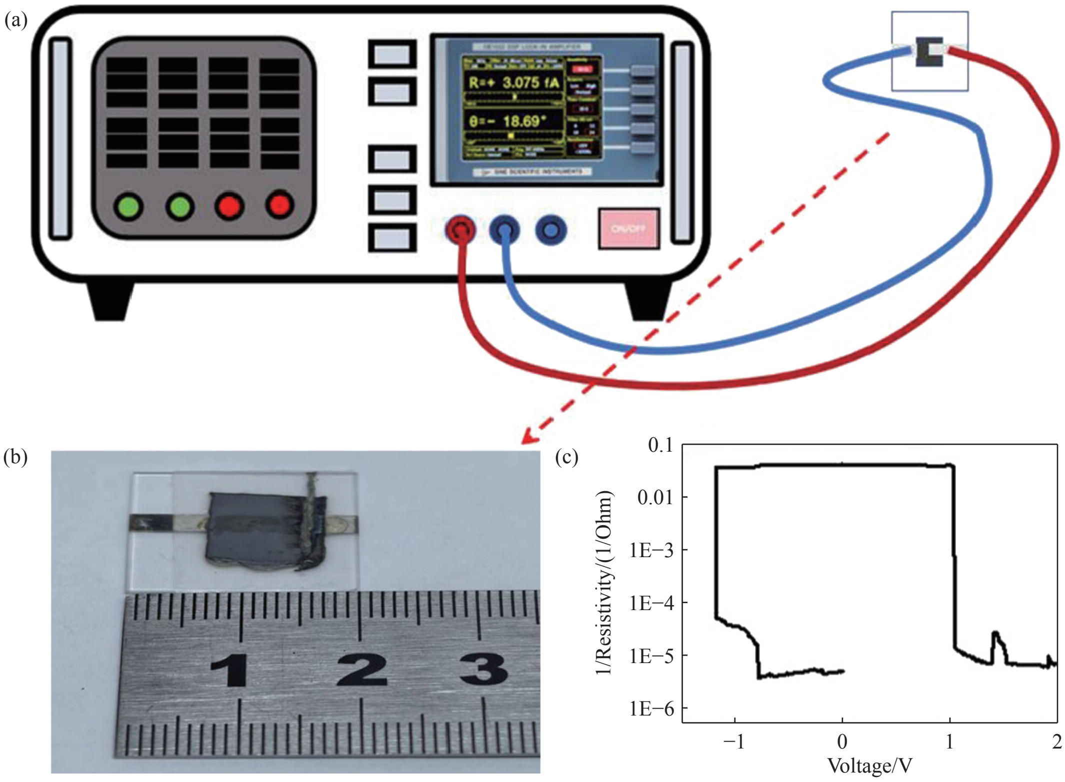

Fig. 2 (a) Schematic of electrical characterization of MoS_2 via digital source table; (b)The resistance measurement sample of a MoS_2 layer with two disconnected silver electrodes; (c)Voltage-dependent resistance data of the MoS_2 layer.

3.2 Performances of the designed metasurface THz modulator

The FDTD Solution is employed to simulate the metasurface micro-nano unit structure with specific dimensions shown in Figure 3a. The frequency-domain results of transmission simulations for the metasurface micro-nano unit structure are presented in Fig. 3b. The analysis reveals that when MoS_2 is in the 2H state, the metasurface exhibits a resonance absorption peak at 0.58 THz; When MoS_2 transforms from the 2H state to the 1T state, the absorption peak shifts to 0.32 THz, leading to the absorption amplitude at 0.58 THz increases from 0.02 to 0.8 as shown in Fig. 3b. This transition results in a highly modulated amplitude at 0.58 THz with a modulation rate of 98% and an insertion loss of only around 20% seen from Fig. 3b. To explain this phenomenon, we analyzed the electric field distribution across the parallel cross-section of the "H" -type silver electrode at 0.58 THz, as shown in Figures 3c and d. When MoS2 is in the 2H phase, it exhibits a high resistance, creating an open circuit in the "H" -type silver electrode gap. The strong field intensity demonstrates intense resonance absorption of the metasurface, corresponding to the absorption peak at 0.58 THz in the frequency-domain spectrum. When MoS_2 transforms to the 1T phase, it enters a low-resistance state, making the open "H" -type silver electrode short-circuit. This leads to a sharp decrease in electric field intensity at the open junction, indicating minimal resonance absorption at this frequency, which corresponds to the increased amplitude observed at 0.58 THz in the spectrum.

Since the designed THz modulator can also be regarded as a grating along the direction of the two parallel legs of the "H" shape, an 18-mm modulation plane composed of 150×150 modulation units which can generate a 1×150 single-row transmission amplitude grating is simulated to validate the diffraction performances of the designed modulator. We simulate terahertz wave diffraction patterns of the designed device with different grating constants of 600, 1 200, and 1 800 μm, respectively. Figures 4a, b, and c show transmission amplitude distributions at these grating constants (only 15 rows of amplitude data are displayed for better visualization). When the grating constant *d* is 600 μm, the device exhibits 30 grating periods, with diffraction angle distributions shown in Figures 4d and g. Results show a first-order diffraction peak at ±58° and no second-order diffraction. At *d*=1 200 μm, the device has 15 grating periods, as shown in Figures 4e and h. This configuration produces a first-order peak at±25°andsecond-orderdiffractionat±58°.For*d*=1 800 μm, the device contains 10 grating periods with diffraction patterns in Figures 4f and i. The results demonstrate a first-order peak at ±16°, second-order diffraction at ±25°, and third-order diffraction at ±58°, respectively.

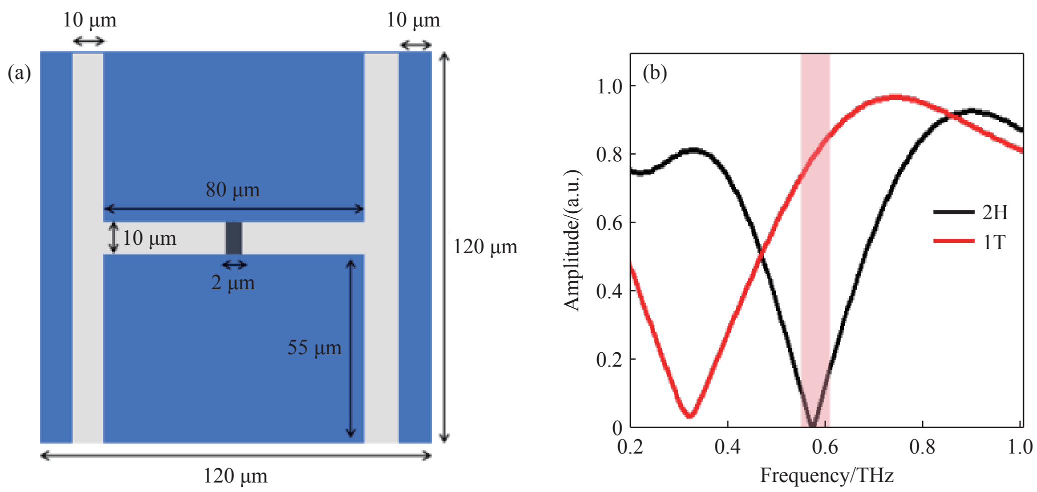

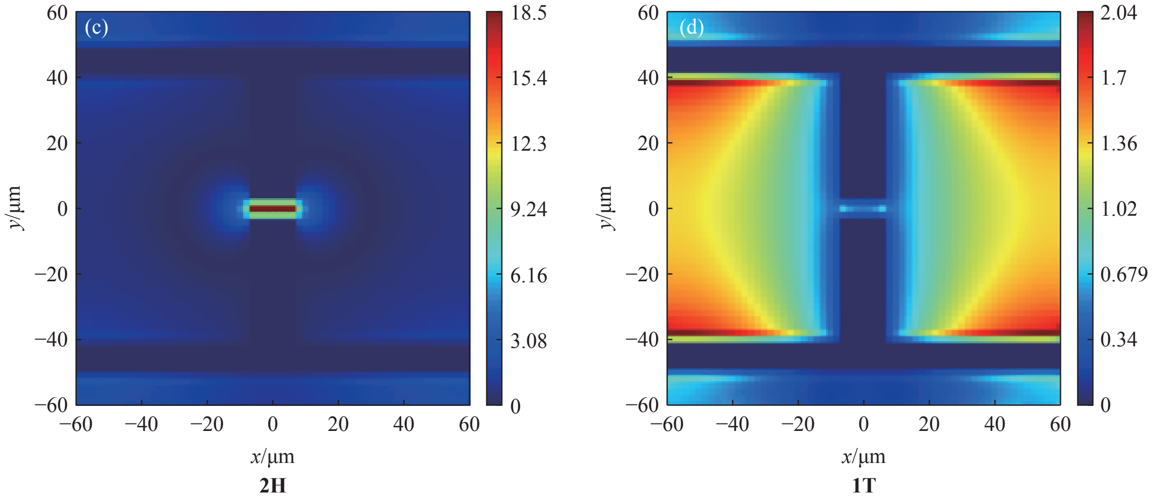

Fig. 3 (a) The unit micro-nanostructure of the electrically controlled MoS_2 metasurface where the white region represents the Ag electrode, the blue region represents the SiO_2 layer under the layer of the Ag electrode and the grey region represents the MoS_2 layer; (b) Resonance spectra of the unit micro-nanostructures before and after the electrical-controlled phase transition (the light red region indicates the operating frequency); (c) Electric field distribution at the interface of the unit micro-nanostructures when MoS_2 is in the 2H phase. (d) Electric field distribution at the interface of the unit micro-nanostructures when MoS_2 is in the 1T phase.

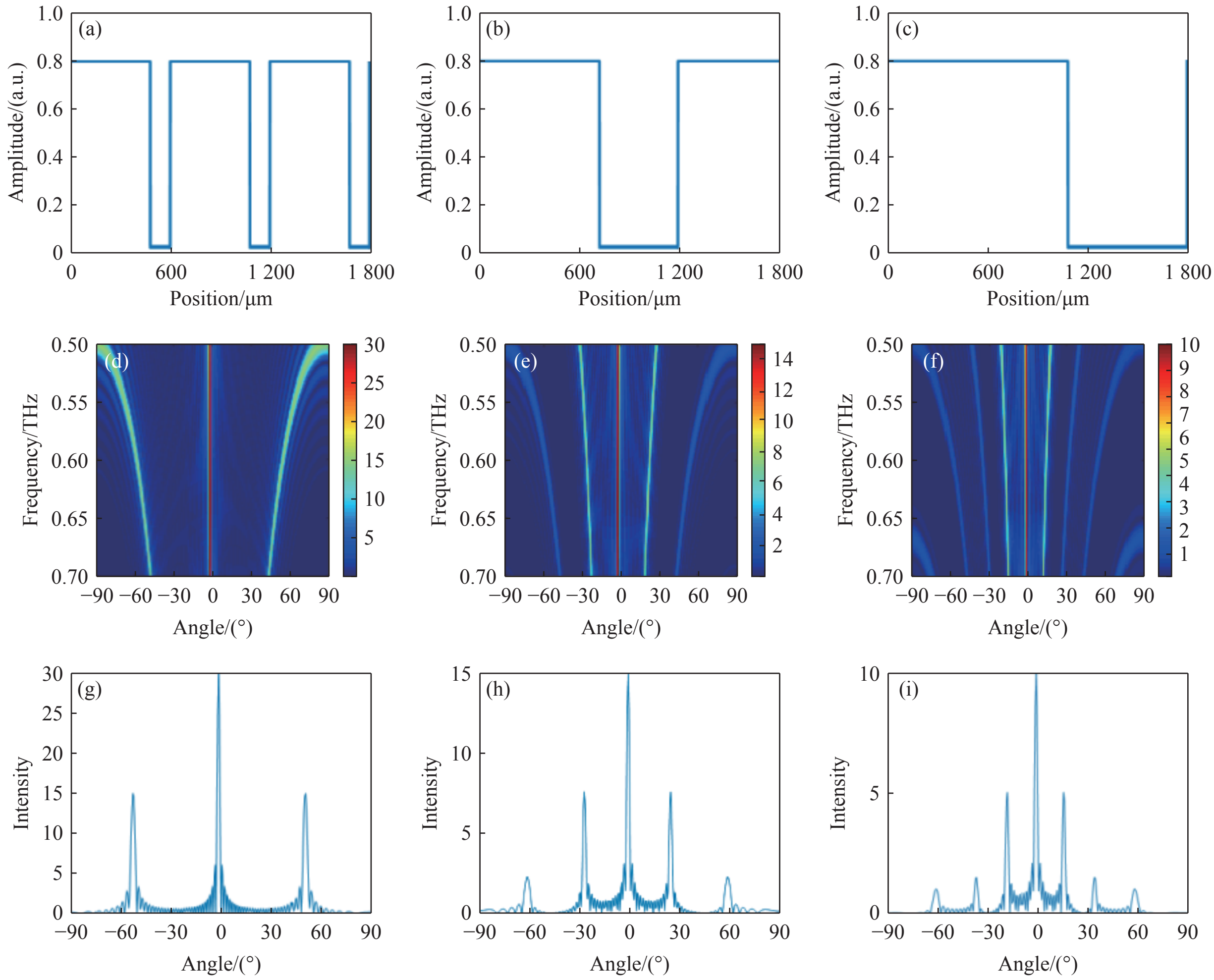

Fig. 4 THz Amplitude variation with position of gratings with different grating constants: (a) 600 μm, (b) 1 200 μm, and (c) 1 800 μm and the corresponding simulated diffraction patterns of frequency (d)-(f) and intensity at 0.58 THz (g)-(i).

4 Conclusion

In this research, an electrically controlled terahertz metasurface was developed based on the phase transition of MoS_2, which was capable of modulating the amplitude of terahertz (THz) wave via an external excitation voltage. The micro-nano unit structure is composed of an "H"-shaped silver electrode with an intermediate gap which is coated with a MoS_2 layer. The electrically controlled phase transition of MoS_2 was measured by means of a digital oscilloscope. Results indicated that MoS_2 could transition from the 2H state to the 1T state under voltage excitation, and the reverse transition occurs when the reverse excitation is applied. Finite element simulations were performed to analyze the frequency-domain amplitude changes of the metasurface before and after the MoS_2 phase transition. A modulation depth of 98% and an insertion loss of 20% were achieved at 0.58 THz. Based on this design, a one-dimensional modulated THz grating with 150 units was fabricated, and the diffraction patterns of the device with different grating constants of 600, 1 200, and 1 800 μm were simulated and different diffraction peaks were observed, respectively. Notably, our metasurface modulator only supports a single resonance at 0.58 THz under the given parameters. Nevertheless, broadband or multi-resonant THz modulators are urgently demanded for THz high-speed communications, real-time imaging, spectroscopy, reconfigurable phased arrays and beam steering systems. Three hierarchical strategies can be adopted to extend modulation bandwidth. At the material level, doping, thinning phase-change films and hybrid integration with 2D materials alleviate intrinsic narrowband dielectric dispersion[46]. Structurally, multi-resonant aperiodic metasurfaces, anti-reflection coatings and cascaded multilayers remove discrete resonant peaks to expand the continuous working spectrum[47]. At the device level, low-parasitic optical pumping paired with low-dispersion THz waveguides eliminates frequency cutoffs and absorption dips, enabling consistent modulation depth and phase shift across an ultrawide THz band[48]. This innovative work is anticipated to promote the development of THz functional devices and offer a novel method for designing electrically controlled THz metasurfaces.

References:

[1] GOPALAN P, SENSALE-RODRIGUEZ B. 2D materials for terahertz modulation[J]. *Advanced Optical Materials*, 2020, 8(3): 1900550.

[2] DEGL'INNOCENTI R, KINDNESS S J, BEERE H E, *et al*.. All-integrated terahertz modulators[J]. *Nanophotonics*, 2018, 7(1): 127-144.

[3] SENSALE-RODRIGUEZ B, YAN R S, RAFIQUE S, *et al*.. Extraordinary control of terahertz beam reflectance in graphene electro-absorption modulators[J]. *Nano Letters*, 2012, 12(9): 4518-4522.

[4] CHEN H T, PADILLA W J, CICH M J, *et al*.. A metamaterial solid-state terahertz phase modulator[J]. *Nature Photonics*, 2009, 3(3): 148-151.

[5] SAVO S, SHREKENHAMER D, PADILLA W J. Liquid crystal metamaterial absorber spatial light modulator for THz applications[J]. *Advanced Optical Materials*, 2014, 2(3): 275-279.

[6] CHIKHI N, LISITSKIY M, PAPARI G, *et al*.. A hybrid tunable THz metadevice using a high birefringence liquid crystal[J]. *Scientific Reports*, 2016, 6(1): 34536.

[7] VASIĆ B, ZOGRAFOPOULOS D C, ISIĆ G, *et al*.. Electrically tunable terahertz polarization converter based on overcoupled metal-isolator-metal metamaterials infiltrated with liquid crystals[J]. *Nanotechnology*, 2017, 28(12): 124002.

[8] NAN T, ZHAO H, GUO J Y, *et al*.. Generation of structured light beams with polarization variation along arbitrary spatial trajectories using tri-layer metasurfaces[J]. *Opto-Electronic Science*, 2024, 3(5): 230052.

[9] KOENIG S, LOPEZ-DIAZ D, ANTES J, *et al*.. Wireless sub-THz communication system with high data rate[J]. *Nature Photonics*, 2013, 7(12): 977-981.

[10] LIAO SH K, CAI W Q, LIU W Y, *et al*.. Satellite-to-ground quantum key distribution[J]. *Nature*, 2017, 549(7670): 43-47.

[11] OSHIMA N, HASHIMOTO K, SUZUKI S, *et al*.. Terahertz wireless data transmission with frequency and polarization division multiplexing using resonant-tunneling-diode oscillators[J]. *IEEE Transactions on Terahertz Science and Technology*, 2017, 7(5): 593-598.

[12] WEN Q Y, TIAN W, MAO Q, *et al*.. Graphene based all-optical spatial terahertz modulator[J]. *Scientific Reports*, 2014, 4(1): 7409.

[13] FERGUSON B, ZHANG X CH. Materials for terahertz science and technology[J]. *Nature Materials*, 2002, 1(1): 26-33.

[14] TONOUCHI M. Cutting-edge terahertz technology[J]. *Nature Photonics*, 2007, 1(2): 97-105.

[15] CHEN H T, PADILLA W J, ZIDE J M O, *et al*.. Active terahertz metamaterial devices[J]. *Nature*, 2006, 444(7119): 597-600.

[16] HENDRY E, GARCIA-VIDAL F J, MARTIN-MORENO L, *et al*.. Optical control over surface-plasmon-polariton-assisted THz transmission through a slit aperture[J]. *Physical Review Letters*, 2008, 100(12): 123901.

[17] ZHAO H, WANG X K, LIU SH T, *et al*.. Highly efficient vectorial field manipulation using a transmitted tri-layer metasurface in the terahertz band[J]. *Opto-Electronic Advances*, 2023, 6(2): 220012.

[18] WANG P L, LOU J, FANG G Y, *et al*.. Progress on cutting-edge infrared-terahertz biophysics[J]. *IEEE Transactions on Microwave Theory and Techniques*, 2022, 70(11): 5117-5140.

[19] HE Y ZH, MA CH SH. Analysis of the effect of antenna pointing error caused by satellite perturbation on space terahertz communication[J]. *Applied Sciences*, 2022, 12(21): 10772.

[20] LV X J, AKO R T, BHASKARAN M, *et al*.. Frequency-selective-surface-based mechanically reconfigurable terahertz bandpass filter[J]. *IEEE Transactions on Terahertz Science and Technology*, 2022, 12(3): 257-266.

[21] LI J T, YUE ZH Y, LI J, *et al*.. Wavefront-controllable all-silicon terahertz meta-polarizer[J]. *Science China Materials*, 2023, 66(1): 300-308.

[22] BUNDEL P, WU G B, CHEN B J, *et al*.. Wideband circular polarizer for a photoconductive antenna[J]. *Optics Letters*, 2023, 48: 3223-3226.

[23] SU H, ZHENG Z S, YU ZH SH, *et al*.. Optically controlling broadband terahertz modulator based on layer-dependent $PtSe_2$ nanofilms[J]. *Nanomaterials*, 2023, 13(5): 795.

[24] GONG S, PING D Y, BI CH Y, *et al*.. High-performance direct terahertz modulator based on resonance mode transformation for high-speed wireless communication[J]. *Applied Physics Letters*, 2022, 121(23): 231104.

[25] TAO SH N, SHEN ZH X, YU H G, *et al*.. Transflective spatial terahertz wave modulator[J]. *Optics Letters*, 2022, 47(7): 1650-1653.

[26] ZHANG P J, CAI T, ZHOU Q L, *et al*.. Ultrahigh modulation enhancement in all-optical Si-based THz modulators integrated with gold nanobipyramids[J]. *Nano Letters*, 2022, 22(4): 1541-1548.

[27] WU Y, LA-O-VORAKIAT C, QIU X P, *et al*.. Graphene terahertz modulators by ionic liquid gating[J]. *Advanced Materials*, 2015, 27(11): 1874-1879.

[28] TAMAGNONE M, FALLAHI A, MOSIG J R, *et al*.. Fundamental limits and near-optimal design of graphene modulators and non-reciprocal devices[J]. *Nature Photonics*, 2014, 8(7): 556-563.

[29] CHEN Z F, CHEN X Q, TAO L, *et al*.. Graphene controlled Brewster angle device for ultra broadband terahertz modulation[J]. *Nature Communications*, 2018, 9(1): 4909.

[30] DI GASPARE A, POGNA E A A, RICCARDI E, *et al*.. All in one-chip, electrolyte-gated graphene amplitude modulator, saturable absorber mirror and metrological frequency-tuner in the 2–5 THz range[J]. *Advanced Optical Materials*, 2022, 10(22): 2200819.

[31] KOSHELEV K, TANG Y T, LI K, *et al*.. Nonlinear metasurfaces governed by bound states in the continuum[J]. *ACS Photonics*, 2019, 6(7): 1639-1644.

[32] HUANG L L, CHEN X ZH, MÜHLENBERND H, *et al*.. Dispersionless phase discontinuities for controlling light propagation[J]. *Nano Letters*, 2012, 12(11): 5750-5755.

[33] HUANG L L, CHEN X ZH, MÜHLENBERND H, *et al*.. Three-dimensional optical holography using a plasmonic metasurface[J]. *Nature Communications*, 2013, 4(1): 2808.

[34] DENG L G, DENG J, GUAN ZH Q, *et al*.. Malus-metasurface-assisted polarization multiplexing[J]. *Light: Science & Applications*, 2020, 9(4): 101.

[35] ZHENG G X, MÜHLENBERND H, KENNEY M, *et al*.. Metasurface holograms reaching 80% efficiency[J]. *Nature Nanotechnology*, 2015, 10(4): 308-312.

[36] TOGNAZZI A, ROCCO D, GANDOLFI M, *et al*.. High quality factor silicon membrane metasurface for intensity-based refractive index sensing[J]. *Optics*, 2021, 2(3): 193-199.

[37] DU K, BARKAOUI H, ZHANG X D, *et al*.. Optical metasurfaces towards multifunctionality and tunability[J]. *Nanophotonics*, 2022, 11(9): 1761-1781.

[38] OU X N, ZENG T B, ZHANG Y, *et al*.. Tunable polarization-multiplexed achromatic dielectric metalens[J]. *Nano Letters*, 2022, 22(24): 10049-10056.

[39] WEN Y F, ZHANG Q, HE Q, *et al*.. Shortening focal length of 100-mm aperture flat lens based on improved sagnac interferometer and bifacial liquid crystal[J]. *Advanced Optical Materials*, 2023, 11(16): 2300127.

[40] HU Y Q, OU X N, ZENG T B, *et al*.. Electrically tunable multifunctional polarization-dependent metasurfaces integrated with liquid crystals in the visible region[J]. *Nano Letters*, 2021, 21(11): 4554-4562.

[41] SABRI R, FOROUZMAND A, MOSALLAEI H. Genetically optimized dual-wavelength all-dielectric metasurface based on double-layer epsilon-near-zero indium-tin-oxide films[J]. *Journal of Applied Physics*, 2020, 128(22): 223101.

[42] CAI Z Q, LIU Y M. Near-infrared reflection modulation through electrical tuning of hybrid graphene metasurfaces[J]. *Advanced Optical Materials*, 2022, 10(6): 2102135.

[43] TIAN J Y, ADAMO G, LIU H L, *et al*.. Phase-change perovskite microlaser with tunable polarization vortex[J]. *Advanced Materials*, 2023, 35(1): 2207430.

[44] XIAO X Y, PENG Z X, ZHANG Z R, *et al*.. Fully printed zero-static power MoS_2 switch coded reconfigurable graphene metasurface for RF/microwave electromagnetic wave manipulation and control[J]. *Nature Communications*, 2024, 15(1): 10591.

[45] HU R J, MIN Q X, LIU X, *et al*.. Terahertz programmable metasurface for phase modulation based on free carrier plasma dispersion effect[J]. *Applied Physics Letters*, 2024, 124(25): 251703.

[46] LIU SH H, CHEN F. Dual-channel dynamically tunable terahertz broadband perfect absorber based on a VO_2 and MoS_2 composite structure[J]. *Physical Chemistry Chemical Physics*, 2026, 28(9): 5807-5818.

[47] LIU T, DAI CH H, WANG D Y, *et al*.. High-efficiency vectorial holography based on ultra-thin metasurfaces[J]. *Advanced Photonics*, 2025, 7(5): 056004.

[48] GUISE J, RATOVO H, FLORES F G P, *et al*.. 1550-nm-pumped InAs-based terahertz modulator integrated in a WR1.0 waveguide[J]. *IEEE Transactions on Terahertz Science and Technology*, 2026, 16(4): 406-416.

Author Biographies：

SHEN Yan-chun (1980—), Male, born in Guangzhou, Guangdong Province, Ph.D. and Professor. His research interest is Terahertz liquid crystal devices. E-mail: shenyanchun@gtxy.edu.cn

WEI Dong-shan (1979—), Male, born in Chibi, Hubei Province, Ph.D., Professor and Doctor's supervisor. His research interests include Terahertz spectroscopy and optoelectric sensing detection technology. Email: dswei@hainnu.edu.cn